Hindawi
Journal of Function Spaces
Volume 2023, Article ID 8883811, 16 pages
https://doi.org/10.1155/2023/8883811

Research Article

Optical Solitons for the Fokas-Lenells Equation with Beta and M-Truncated Derivatives

Farah M. Al-Askar

Department of Mathematical Science, College of Science, Princess Nourah bint Abdulrahman University, P.O. Box 84428, Riyadh 11671, Saudi Arabia

Correspondence should be addressed to Farah M. Al-Askar; famalaskar@pnu.edu.sa

Received 3 July 2023; Revised 25 September 2023; Accepted 19 October 2023; Published 16 November 2023

Academic Editor: Shrideh K. Q. Al-Omari

The Fokas-Lenells equation (FLE) including the M-truncated derivative or beta derivative is examined. Using the modified mapping method, new elliptic, hyperbolic, rational, and trigonometric solutions are created. Also, we extend some previous results. Since the FLE has various applications in telecommunication modes, quantum field theory, quantum mechanics, and complex system theory, the solutions produced may be used to interpret a broad variety of important physical process. We present some of 3D and 2D diagrams to illustrate how M-truncated derivative and the beta derivative influence the exact solutions of the FLE. We demonstrate that when the derivative order decreases, the beta derivative pushes the surface to the left, whereas the M-truncated derivative pushes the surface to the right.

1. Introduction

Nonlinear evolution equations (NEEs) have a broad application in engineering and scientific areas, such as chemical kinematics, heat flow, fluid mechanics, optical fibers, wave propagation phenomena, solid-state physics, shallow water wave propagation, and quantum mechanics. Obtaining traveling wave solutions is one of the crucial physical problems for NEEs. Consequently, in nonlinear sciences, the search for mathematical approaches for creating the analytical solutions to NEEs is currently a crucial and vital task. In recent years, numerous techniques for addressing NEEs have been developed, including F-expansion technique [1], spectral methods [2], $\exp(-\phi(\varsigma))$-expansion [3], tanh-sech method [4], Hirota's method [5], extended trial equation [6], extended tanh-coth method [7, 8], Lie's symmetry analysis [9–11], He's semi-inverse method [12], generalized exponential rational function [13], generalized Riccati simplest equation [14, 15], new auxiliary equation approach [16], perturbation method [17], (G'/G)-expansion [18, 19], improved Sardar subequation [20], Jacobi elliptic function [21, 22], modified simple equation method [23], and more recent techniques.

One of the most important of NEEs is the Fokas-Lenells equation (FLE) [24–26]:

$$\Phi_{tx} - \gamma_1 \Phi_{xx} - 2i\gamma_2 \Phi_x + \vartheta |\Phi|^2 (\Phi + i\rho \Phi_x) = 0, \tag{1}$$

where $\Phi(x,t)$ describes the complex field, $i = \sqrt{-1}$, $\vartheta = \pm 1$, and γ_1, γ_2, and ρ are the positive constants. Equation (1) has various applications in complex system theory, quantum field theory, telecommunication, and quantum mechanics models. Moreover, it occurs as a pattern that indicates the propagation of nonlinear pulses in optical fibers. Many researchers have obtained the exact solutions of Eq. (1) by employing several methods such as the generalized Kudryashov and extended trial equation methods [24], Riccati's equation method [27], $(m + 1/G')$-expansion method [28], complex envelope function ansatz [29], and mapping method [30].

In this study, we consider Eq. (1) with two different time derivative operators as follows:

With beta derivative operator, Eq. (1) takes the form

$$\mathscr{D}_t^{\alpha}\Phi_x - \gamma_1\Phi_{xx} - 2i\gamma_2\Phi_x + \vartheta|\Phi|^2(\Phi + i\rho\Phi_x) = 0, \quad (2)$$

where $\mathscr{D}_t^{\alpha}$ is the beta derivative (BD) operator.

And with M-truncated derivative operator, Eq. (1) takes the form

$$\mathscr{D}_{m,t}^{\alpha,\sigma}\Phi_x - \gamma_1\Phi_{xx} - 2i\gamma_2\Phi_x + \vartheta|\Phi|^2(\Phi + i\rho\Phi_x) = 0, \quad (3)$$

where $\mathscr{D}_{m,t}^{\alpha,\sigma}$ is the M-truncated derivative (MTD) operator.

The novelty of this study is to find of the exact solutions of FLE (2) and (3). In order to reach these solutions, we use a modified mapping method (MM-method). We extend some previous results such as [24, 27]. Using the BD in Eq. (2) and the MTD in Eq. (3), the solutions would be very helpful to physicists in characterizing a wide variety of important physical processes. To further explore the effect of the BD and MTD on the acquired solution of FLE (2) and (3), we present some figures constructed in MATLAB.

The study's structure is as follows: In Section 2, we define the BD and MTD and state their prosperities. In Section 3, we explain the modified mapping method, while the wave equation of FLE-MTD (2) is obtained in Section 4. In Section 5, we get the exact solutions of the FLE-MTD (2). In Section 6, we can observe how the BD and MTD affect the obtained solutions of FLE-MTD (2). Lastly, the findings of the study are given.

2. Preliminaries

Recently, the fractional NEEs have increased in popularity owing to their broad variety of applications in domains such as biological population, signal processing, plasma physics, electrical networks, fluid flow, solid state, finance, chemical kinematics, optical fiber, and control theory physics. Various types of fractional derivatives were introduced by different mathematicians. The most prominent are those suggested by Caputo, Grunwald-Letnikov, Hadamard, Erdelyi, Riemann-Liouville, Marchaud, and Riesz [31–34]. The bulk of fractional derivatives does not involve the standard derivative rules including the product rule, chain rule, and quotient rule.

2.1. Beta Derivative. Atangana et al. [35] developed a novel operator derivative known as BD. The BD [35] is defined for $u : (0,\infty) \longrightarrow \mathbb{R}$ as

$$\mathscr{D}_t^{\alpha}u(t) = \lim_{h\longrightarrow 0}\frac{u\left(t + h(t + (1/\Gamma(\alpha)))^{1-\alpha}\right) - u(t)}{h}, \quad 0 < \alpha \le 1. \quad (4)$$

Moreover, for any constants a and b, the BD has the following features [35]:

$$\begin{aligned}
\mathscr{D}_t^{\alpha}u(t) &= \left(t + \frac{1}{\Gamma(\alpha)}\right)^{1-\alpha}\frac{du}{dt},\\
\mathscr{D}_t^{\alpha}(au + bv) &= a\mathscr{D}_t^{\alpha}(u) + b\mathscr{D}_t^{\alpha}(v),\\
\mathscr{D}_t^{\alpha}(a) &= 0,\\
\mathscr{D}_t^{\alpha}(t^m) &= \left(t + \frac{1}{\Gamma(\alpha)}\right)^{1-\alpha}t^{m-\alpha},\\
\mathscr{D}_t^{\alpha}(u\circ v(t)) &= v'(t)\mathscr{D}_t^{\alpha}(u(v(t))).
\end{aligned} \quad (5)$$

2.2. M-Truncated Derivative. Sousa and de Oliveira [36] proposed another derivative known as the MTD. The MTD of order $\alpha \in (0, 1]$ is defined as

$$\mathscr{D}_{m,t}^{\alpha,\sigma}u(t) = \lim_{h\longrightarrow 0}\frac{u(t\mathscr{E}_{m,\sigma}(ht^{-\alpha})) - u(t)}{h}, \quad (6)$$

where

$$\mathscr{E}_{m,\sigma}(y) = \sum_{k=0}^{m}\frac{y^k}{\Gamma(\sigma k + 1)}, \text{ for } \sigma > 0 \text{ and } y \in \mathbb{C}. \quad (7)$$

The MTD satisfies the following characteristics [36]:

$$\begin{aligned}
\mathscr{D}_{m,t}^{\alpha,\sigma}(au + bv) &= a\mathscr{D}_{m,t}^{\alpha,\sigma}(u) + b\mathscr{D}_{m,t}^{\alpha,\sigma}(v),\\
\mathscr{D}_{m,t}^{\alpha,\sigma}(u\circ v)(z) &= u'(v(z))\mathscr{D}_{m,t}^{\alpha,\sigma}v(z),\\
\mathscr{D}_{m,t}^{\alpha,\sigma}(uv) &= u\mathscr{D}_{m,t}^{\alpha,\sigma}v + v\mathscr{D}_{m,t}^{\alpha,\sigma}u,\\
\mathscr{D}_{m,t}^{\alpha,\sigma}(u)(t) &= \frac{t^{1-\alpha}}{\Gamma(\sigma+1)}\frac{du}{dt},\\
\mathscr{D}_{m,t}^{\alpha,\sigma}(t^v) &= \frac{v}{\Gamma(\sigma+1)}t^{v-\alpha}.
\end{aligned} \quad (8)$$

3. The Clarification of MM-Method

Here, we implement the MM-method from [37]. Let the solutions to Eq. (19) take the form

$$\Psi(\eta) = \sum_{i=0}^{M}\ell_i\varphi^i(\eta) + \sum_{i=1}^{M}\hbar_i\varphi^{-i}(\eta), \quad (9)$$

where ℓ_j and $\hbar_j$ are the undetermined constants for $j = 1, 2, .., M$ and φ solves

$$\varphi' = \sqrt{r + q\varphi^2 + p\varphi^4}, \quad (10)$$

where the constants r, q, and p are real numbers. Equation (10) has different solutions for r, p, and q as follows:

$sn(\eta) = sn(\eta,\kappa)$,$dn(\eta,\kappa) = dn(\eta,\kappa)$, and $cn(\eta) = cn(\eta,\kappa)$ are the Jacobi elliptic functions (JEFs) for $0 < \kappa < 1$. When

Table 1: All solutions for Eq. (10) for different r, p, and q.

Case	p	q	r	$\varphi(\eta)$
1	κ^2	$-(1+\kappa^2)$	1	$sn(\eta)$
2	1	$2\kappa^2-1$	$-\kappa^2(1-\kappa^2)$	$ds(\eta)$
3	1	$2-\kappa^2$	$(1-\kappa^2)$	$cs(\eta)$
4	$\kappa^2/4$	$(\kappa^2-2)/2$	1/4	$sn(\eta)/1+dn(\eta)$
5	$(1-\kappa^2)^2/4$	$(1-\kappa^2)^2/2$	1/4	$sn(\eta)/dn+cn(\eta)$
6	$1-\kappa^2/4$	$(1-\kappa^2)/2$	$(1-\kappa^2)/4$	$cn(\eta)/1+sn(\eta)$
7	1	0	0	c/η
8	−1	$2-\kappa^2$	(κ^2-1)	$dn(\eta)$
9	$-\kappa^2$	$2\kappa^2-1$	$(1-\kappa^2)$	$cn(\eta)$
10	$\kappa^2-1/4$	$(\kappa^2+1)/2$	$(\kappa^2-1)/4$	$dn(\eta)/1+sn(\eta)$
11	−1/4	$(\kappa^2+1)/2$	$-(1-\kappa^2)^2/4$	$\kappa cn(\eta)\pm dn(\eta)$

$\kappa \longrightarrow 1$, the following hyperbolic functions are produced from JEFs:

$$cn(\eta)\longrightarrow \operatorname{sech}(\eta), sn(\eta)\longrightarrow \tanh(\eta), cs(\eta)\longrightarrow \operatorname{csch}(\eta),$$
$$dn(\eta)\longrightarrow \operatorname{sech}(\eta), ds\longrightarrow \operatorname{csch}(\eta). \tag{11}$$

Moreover, when $\kappa \longrightarrow 0$, the following trigonometric functions are produced from JEFs:

$$\begin{aligned} cn(\eta) &\longrightarrow \cos(\eta),\\ cs(\eta) &\longrightarrow \cot(\eta),\\ ds &\longrightarrow \operatorname{csc}(\eta),\\ sn(\eta) &\longrightarrow \sin(\eta),\\ dn(\eta) &\longrightarrow 1. \end{aligned} \tag{12}$$

4. Traveling Wave Equation for FLE

To get the wave equation for FLE (2)/(3), we use

$$\Phi(x,t)=\Psi(\eta_\alpha)e^{i\mu_\alpha}, \tag{13}$$

where Ψ is a real function and η_α and μ_α are defined as follows:

(i) In terms of beta derivative

$$\mu_\alpha=\mu_1 x+\frac{\mu_2}{\alpha}\left(t+\frac{1}{\Gamma(\alpha)}\right)^\alpha \text{ and } \eta_\alpha=\eta_1 x+\frac{\eta_2}{\alpha}\left(t+\frac{1}{\Gamma(\alpha)}\right)^\alpha. \tag{14}$$

(ii) In terms of M-truncated derivative

$$\begin{aligned} \mu_\alpha &= \mu_1 x+\frac{\mu_2\Gamma(\sigma+1)}{\alpha}t^\alpha,\\ \eta_\alpha &= \eta_1 x+\frac{\eta_2\Gamma(\sigma+1)}{\alpha}t^\alpha, \end{aligned} \tag{15}$$

where μ_1, μ_2, η_1, and η_2 are the nondefined constants. Putting Eq. (13) into Eq. (2)/(3), we have the following system:

$$(\eta_1\eta_2-\gamma_1\eta_1^2)\Psi''+(\nu-\mu_1\mu_2+\gamma_1^2\mu_1+2\gamma_2\mu_1)\Psi-\nu\rho\mu_1\Psi^3=0, \tag{16}$$

$$i\left[(\eta_1\mu_2+\mu_1\eta_2-2\gamma_1\mu_1\eta_1-2\gamma_2\eta_1)\Psi'+\nu\rho\eta_1\Psi^2\Psi'\right]=0. \tag{17}$$

From imaginary part (17), we obtained

$$\eta_2=\frac{1}{\mu_1}\left(-\eta_1\mu_2+2\gamma_1\mu_1\eta_1+2\gamma_2\eta_1-\nu\rho\eta_1\Psi^2\right), \tag{18}$$

while the real part is given by

$$\Psi''+A\Psi-B\Psi^3=0, \tag{19}$$

where

$$\begin{aligned} A &= \frac{(\nu-\mu_1\mu_2+\gamma_1^2\mu_1+2\gamma_2\mu_1)}{(\eta_1\eta_2-\gamma_1\eta_1^2)},\\ B &= \frac{\nu\rho\mu_1}{(\eta_1\eta_2-\gamma_1\eta_1^2)}. \end{aligned} \tag{20}$$

5. Exact Solutions of FLE

To determine the value of M defined in Eq. (9), we balance Ψ^3 with Ψ'' in Eq. (19) as

$$3M=M+2\Rightarrow M=1. \tag{21}$$

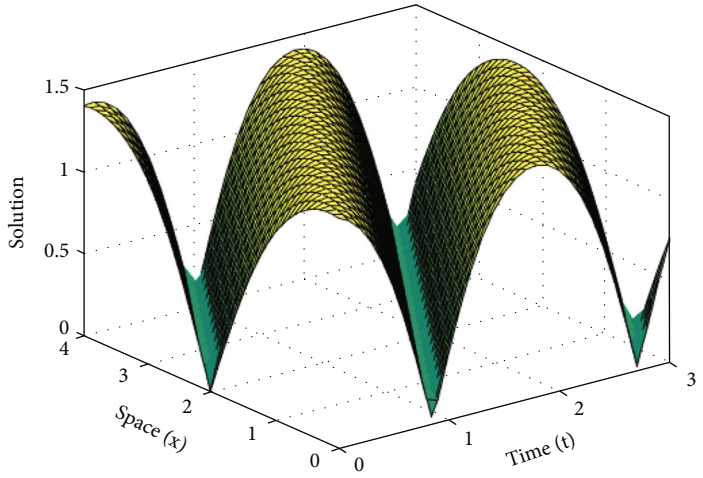

(a) $\alpha = 1$

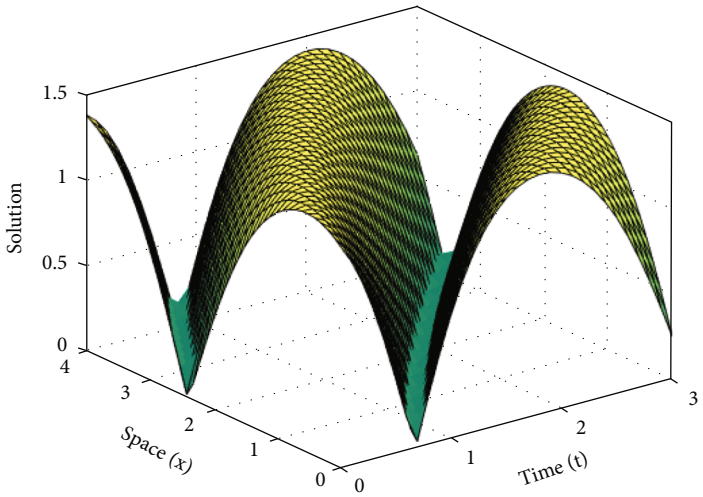

(b) $\alpha = 0.7$

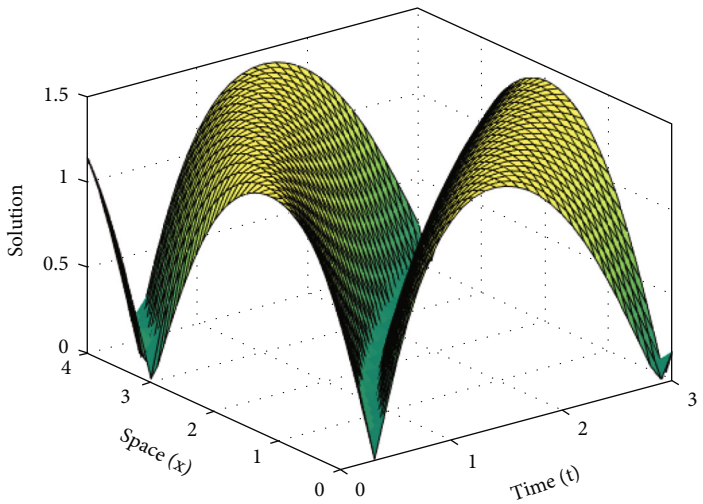

(c) $\alpha = 0.5$

Figure 1: Continued.

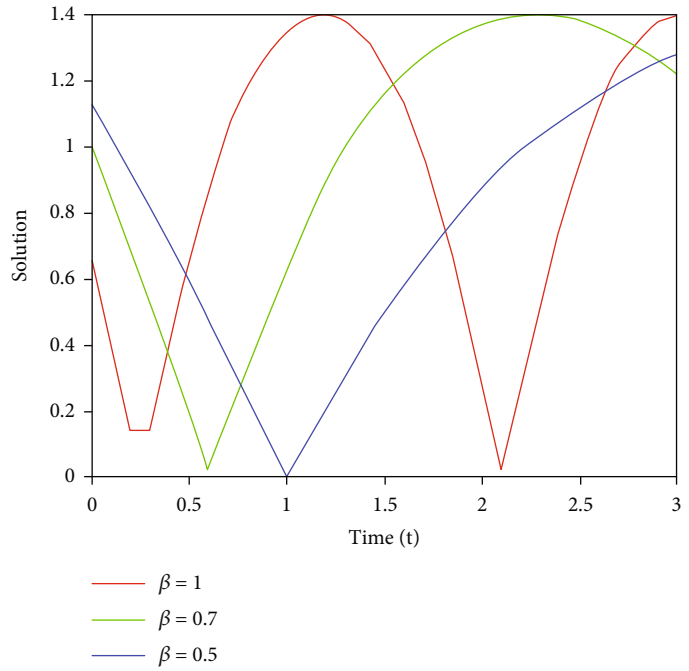

(d) $\alpha = 0.5$, 0.7, and 1

FIGURE 1: (a–c) 3D shape of Eq. (29) with $\alpha = 0.5$, 0.7, and 1. (d) 2D shape of Eq. (29) with distinct values of α.

With $M = 1$, Eq. (9) becomes

$$\Psi(\eta_\alpha) = \ell_0 + \ell_1\varphi(\eta_\alpha) + \frac{\hbar_1}{\varphi(\eta_\alpha)}. \tag{22}$$

Putting Eq. (22) into Eq. (19), we have

$$\begin{aligned}&\left(2\ell_1 p - B\ell_1^3\right)\varphi^3 - 3B\ell_0\ell_1^2\varphi^2 + \left(\ell_1 q - 3B\ell_0^2\ell_1 - 3B\hbar_1\ell_1^2 + \ell_1 A\right)\varphi\\ &+ \left(A\ell_0 - B\ell_0^3 - 6B\ell_0\ell_1\hbar_1\right) + \left(A\hbar_1 + \hbar_1 q - 3B\ell_0^2\hbar_1 - 3B\ell_1\hbar_1^2\right)\varphi^{-1}\\ &- 3B\hbar_1^2\varphi^{-2} + \left(2r\hbar_1 - B\hbar_1^3\right)\varphi^{-3} = 0.\end{aligned} \tag{23}$$

Setting all coefficient of φ^{-k} and φ^k in Eq. (23) be zero for $k = 3, 2, 1, 0$, we get

$$\begin{aligned}2\ell_1 p - B\ell_1^3 &= 0,\\ -3B\ell_0\ell_1^2 &= 0,\\ \ell_1 q - 3B\ell_0^2\ell_1 - 3B\hbar_1\ell_1^2 + \ell_1 A &= 0,\\ A\ell_0 - B\ell_0^3 - 6B\ell_0\ell_1\hbar_1 &= 0,\\ A\hbar_1 + \hbar_1 q - 3B\ell_0^2\hbar_1 - 3B\ell_1\hbar_1^2 &= 0,\\ -3B\ell_0\hbar_1^2 &= 0,\\ 2r\hbar_1 - B\hbar_1^3 &= 0.\end{aligned} \tag{24}$$

There are three sets derived from these equations:

Set 1

$$\begin{aligned}\ell_0 &= 0,\\ \ell_1 &= \pm\sqrt{\frac{2p}{B}},\\ \hbar_1 &= 0,\\ q &= -A.\end{aligned} \tag{25}$$

Set 2

$$\begin{aligned}\ell_0 &= 0,\\ \ell_1 &= 0,\\ \hbar_1 &= \pm\sqrt{\frac{2r}{B}},\\ q &= -A.\end{aligned} \tag{26}$$

Set 3

$$\begin{aligned}\ell_0 &= 0,\\ \ell_1 &= \pm\sqrt{\frac{2p}{B}},\\ \hbar_1 &= \pm\sqrt{\frac{2r}{B}},\\ q &= 6\sqrt{pr} - A.\end{aligned} \tag{27}$$

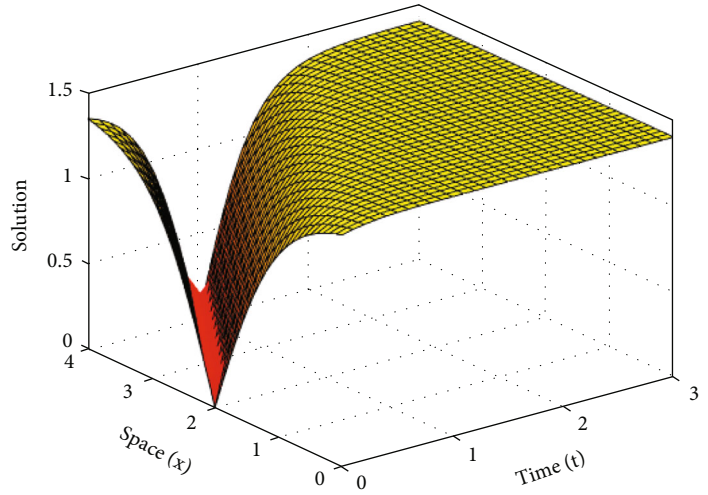

(a) $\alpha = 1$

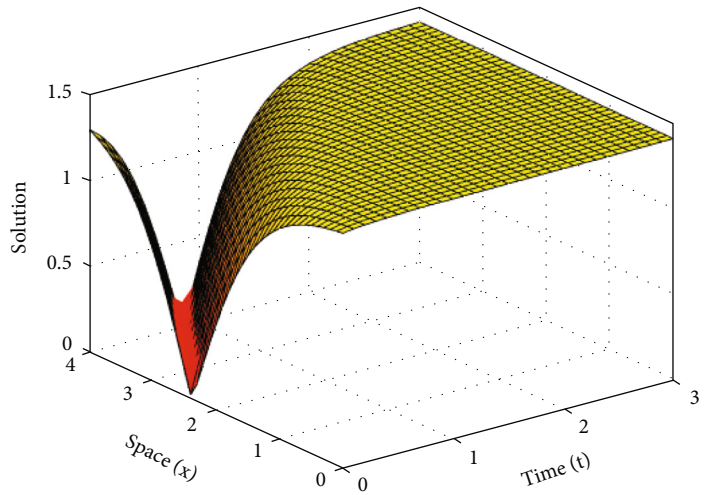

(b) $\alpha = 0.7$

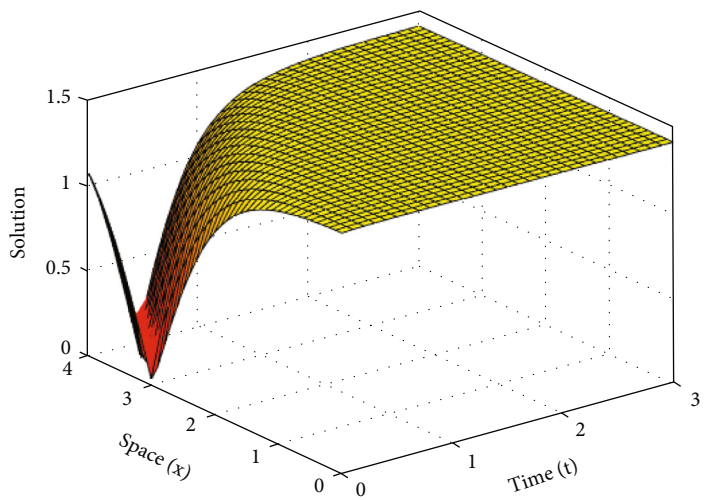

(c) $\alpha = 0.5$

Figure 2: Continued.

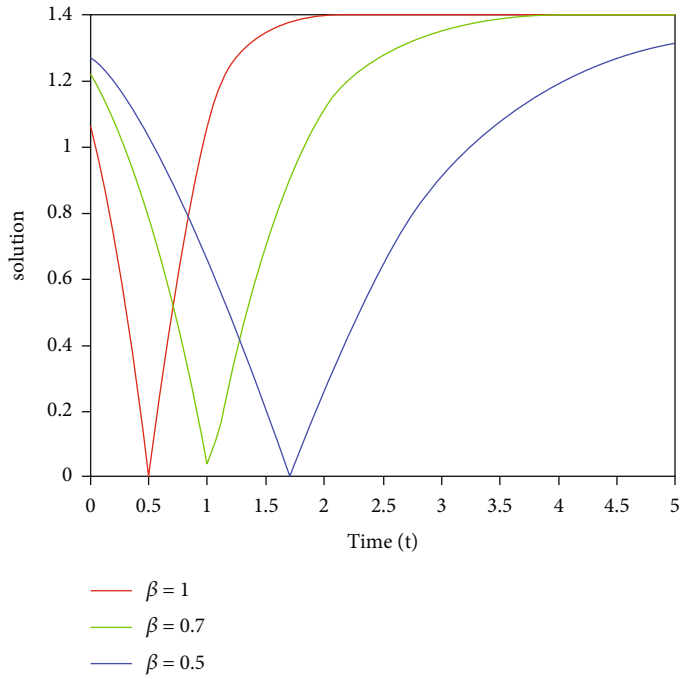

(d) $\alpha = 0.5$, 0.7, and 1

FIGURE 2: (a–c) 3D shape of Eq. (40) with $\alpha = 0.5$, 0.7, and 1. (d) 2D shape of Eq. (40) for distinct values of α.

Set 1. The solution of Eq. (19), utilizing Eqs. (22) and (25), takes the form

$$\Psi(\eta_\alpha) = \pm\sqrt{\frac{2p}{B}}\varphi(\eta_\alpha), \text{for} \frac{p}{B} > 0. \tag{28}$$

Therefore, the solutions of FLE (2)/(3), by using Table 1, are as follows:

Elliptic solutions

$$\Phi(x,t) = \pm\kappa\sqrt{\frac{2}{B}}sn(\eta_\alpha)e^{i\mu_\alpha}, \text{for } B > 0, \tag{29}$$

$$\Phi(x,t) = \pm\sqrt{\frac{2}{B}}ds(\eta_\alpha)e^{i\mu_\alpha}, \text{for } B > 0, \tag{30}$$

$$\Phi(x,t) = \pm\sqrt{\frac{2}{B}}cs(\eta_\alpha)e^{i\mu_\alpha}, \text{for } B > 0, \tag{31}$$

$$\Phi(x,t) = \pm\kappa\sqrt{\frac{1}{2B}}\frac{sn(\eta_\alpha)}{1+dn(\eta_\alpha)}e^{i\mu_\alpha}, \text{for } B > 0, \tag{32}$$

$$\Phi(x,t) = \pm\sqrt{\frac{1}{2B}}\left[\frac{(1-\kappa^2)sn(\eta_\alpha)}{dn(\eta_\alpha)+cn(\eta_\alpha)}\right]e^{i\mu_\alpha}, \text{for } B > 0, \tag{33}$$

$$\Phi(x,t) = \pm\sqrt{\frac{2}{B}\frac{cn(\eta_\alpha)}{1+sn(\eta_\alpha)}}\Bigg]e^{i\mu_\alpha}, \text{for } B > 0, \tag{34}$$

$$\Phi(x,t) = \pm\sqrt{\frac{-2}{B}}dn(\eta_\alpha)e^{i\mu_\alpha}, \text{for } B < 0, \tag{35}$$

$$\Phi(x,t) = \pm\sqrt{\frac{-2\kappa^2}{B}}cn(\eta_\alpha)e^{i\mu_\alpha}, \text{for } B < 0, \tag{36}$$

$$\Phi(x,t) = \pm\sqrt{\frac{(\kappa^2-1)}{2B}\frac{dn(\eta_\alpha)}{1+sn(\eta_\alpha)}}\Bigg]e^{i\mu_\alpha}, \text{for } B < 0, \tag{37}$$

$$\Phi(x,t) = \pm\sqrt{\frac{-1}{2B}}\left[\kappa cn(\eta_\alpha) \pm dn((\eta_\alpha))\right]e^{i\mu_\alpha}, \text{for } B < 0. \tag{38}$$

Rational solutions

$$\Phi(x,t) = \pm\sqrt{\frac{2}{B}\frac{c}{(\eta_\alpha)}}\Bigg]e^{i\mu_\alpha}, \text{for} B > 0. \tag{39}$$

Hyperbolic solutions (if $\kappa \longrightarrow 1$ in (29)-(43))

$$\Phi(x,t) = \pm\sqrt{\frac{2}{B}}\tanh(\eta_\alpha)e^{i\mu_\alpha}, \text{for } B > 0, \tag{40}$$

$$\Phi(x,t) = \pm\sqrt{\frac{2}{B}}\operatorname{csch}(\eta_\alpha)e^{i\mu_\alpha}, \text{for } B > 0, \tag{41}$$

$$\Phi(x,t) = \pm\sqrt{\frac{1}{2B}}\frac{\tanh(\eta_\alpha)}{1+\operatorname{sech}(\eta_\alpha)}e^{i\mu_\alpha}, \text{for } B > 0, \tag{42}$$

$$\Phi(x,t) = \pm\sqrt{\frac{-2}{B}}\operatorname{sech}(\eta_\alpha)e^{i\mu_\alpha}, \text{for } B < 0. \tag{43}$$

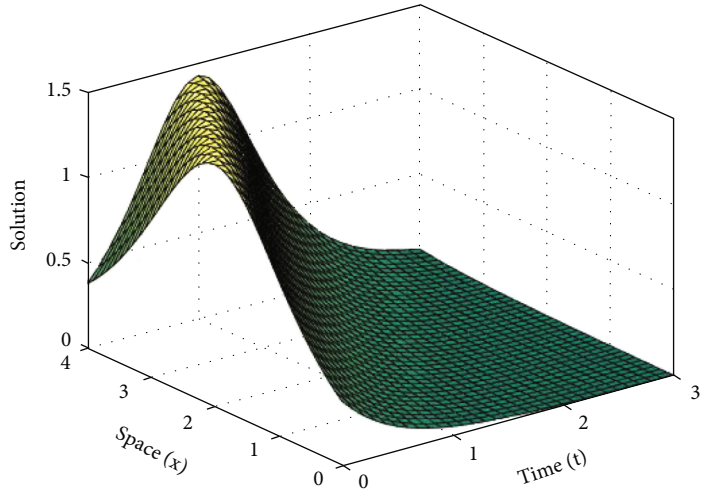

(a) $\alpha = 1$

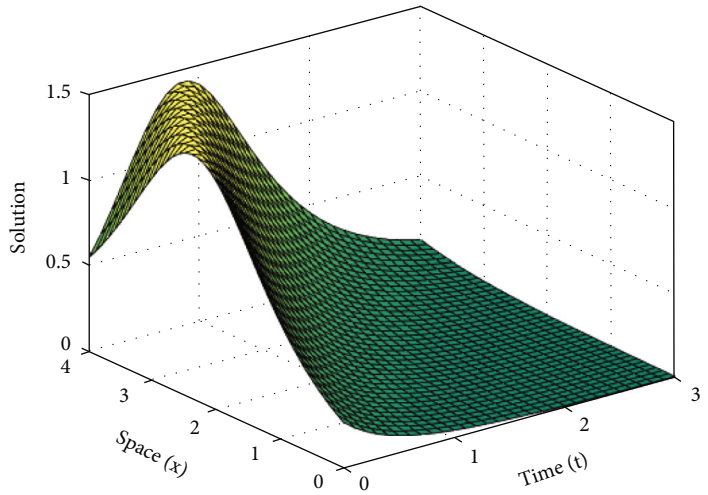

(b) $\alpha = 0.7$

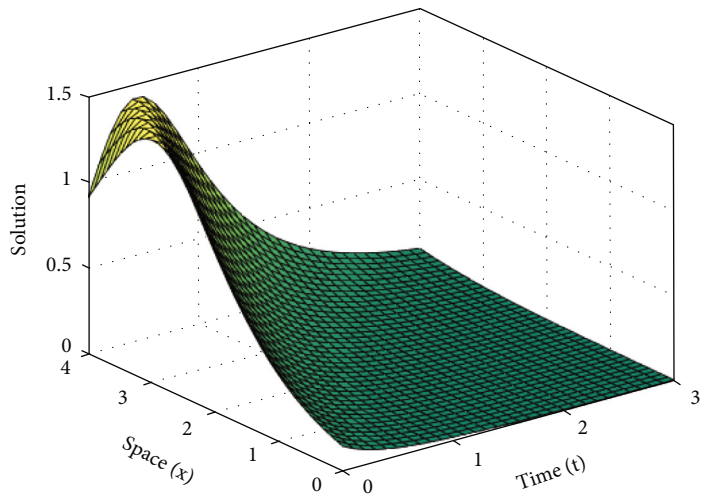

(c) $\alpha = 0.5$

Figure 3: Continued.

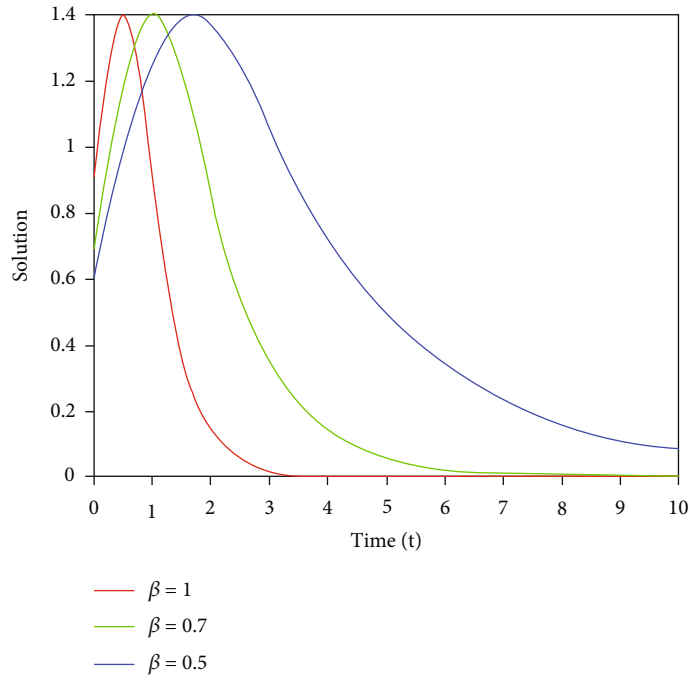

(d) $\alpha = 0.5$, 0.7, and 1

FIGURE 3: (a–c) 3D shape of Eq. (43) with $\alpha = 0.5$, 0.7, and 1. (d) 2D shape of Eq. (43) for various values of α.

Trigonometric solutions (if $\kappa \longrightarrow 0$ in (29)-(43))

$$\Phi(x,t) = \pm\sqrt{\frac{2}{B}}\csc(\eta_\alpha)e^{i\mu_\alpha}, \text{ for } B > 0, \tag{44}$$

$$\Phi(x,t) = \pm\sqrt{\frac{2}{B}}\cot(\eta_\alpha)e^{i\mu_\alpha}, \text{ for } B > 0, \tag{45}$$

$$\Phi(x,t) = \pm\sqrt{\frac{1}{2B}}\left[\frac{\sin(\eta_\alpha)}{1+\cos(\eta_\alpha)}\right]e^{i\mu_\alpha}, \text{ for } B > 0, \tag{46}$$

$$\Phi(x,t) = \pm\frac{1}{2}\sqrt{\frac{2}{B}}\left[\frac{\cos(\eta_\alpha)}{1+\sin(\eta_\alpha)}\right]e^{i\mu_\alpha}, \text{ for } B > 0, \tag{47}$$

$$\Phi(x,t) = \pm\sqrt{\frac{-1}{2B}}\left[\frac{1}{1+\sin(\eta_\alpha)}\right]e^{i\mu_\alpha}, \text{ for } B < 0, \tag{48}$$

where μ_α and η_α are defined in (14) or (15) in the sense of BD or MTD, respectively

Set 2. The solution of Eq. (19), utilizing Eqs. (22) and (26), is

$$\Psi(\eta_\alpha) = \pm\sqrt{\frac{2r}{B}}\frac{1}{\varphi(\eta_\alpha)}, \text{ for } \frac{r}{B} > 0. \tag{49}$$

Therefore, the solutions of FLE (2)/(3), by using Table 1, are as follows:

Elliptic solutions

$$\Phi(x,t) = \pm\sqrt{\frac{2}{B}}\frac{1}{sn(\eta_\alpha)}e^{i\mu_\alpha}, \text{ for } B > 0, \tag{50}$$

$$\Phi(x,t) = \pm\sqrt{\frac{2(1-\kappa^2)}{B}}\frac{1}{cs(\eta_\alpha)}e^{i\mu_\alpha}, \text{ for } B > 0, \tag{51}$$

$$\Phi(x,t) = \pm\sqrt{\frac{2(1-\kappa^2)}{B}}\frac{1}{cn(\eta_\alpha)}e^{i\mu_\alpha}, \text{ for } B > 0, \tag{52}$$

$$\Phi(x,t) = \pm\sqrt{\frac{1}{2B}}\frac{1+dn(\eta_\alpha)}{sn(\eta_\alpha)}e^{i\mu_\alpha}, \text{ for } B > 0, \tag{53}$$

$$\Phi(x,t) = \pm\sqrt{\frac{1-\kappa^2}{2B}}\left[\frac{1+sn(\eta_\alpha)}{cn(\eta_\alpha)}\right]e^{i\mu_\alpha}, \text{ for } B > 0, \tag{54}$$

$$\Phi(x,t) = \pm\sqrt{\frac{1}{2B}}\left[\frac{dn(\eta_\alpha)+cn(\eta_\alpha)}{sn(\eta_\alpha)}\right]e^{i\mu_\alpha}, \text{ for } B > 0, \tag{55}$$

$$\Phi(x,t) = \pm\sqrt{\frac{-2\kappa^2(1-\kappa^2)}{B}}\left[\frac{1}{ds(\eta_\alpha)}\right]e^{i\mu_\alpha}, \text{ for } B < 0, \tag{56}$$

$$\Phi(x,t) = \pm\sqrt{\frac{2(\kappa^2-1)}{B}}\frac{1}{dn(\eta_\alpha)}e^{i\mu_\alpha}, \text{ for } B < 0, \tag{57}$$

$$\Phi(x,t) = \pm\sqrt{\frac{(\kappa^2-1)}{2B}}\left[\frac{1+sn(\eta_\alpha)}{dn(\eta_\alpha)}\right]e^{i\mu_\alpha}, \text{ for } B < 0, \tag{58}$$

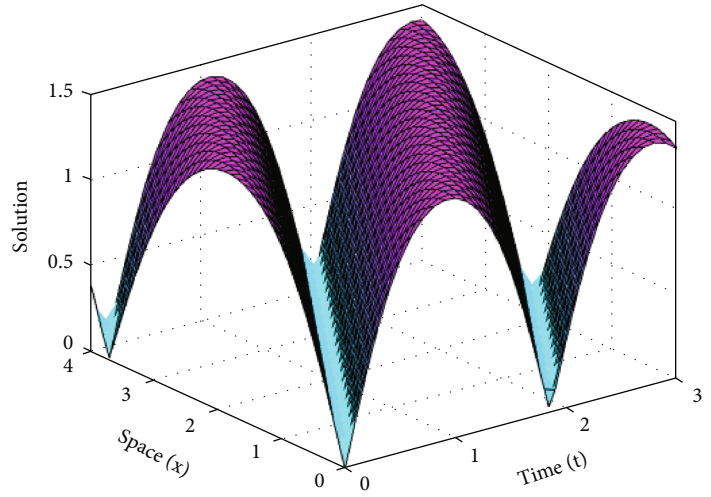

(a) $\alpha = 1, \sigma = 0$

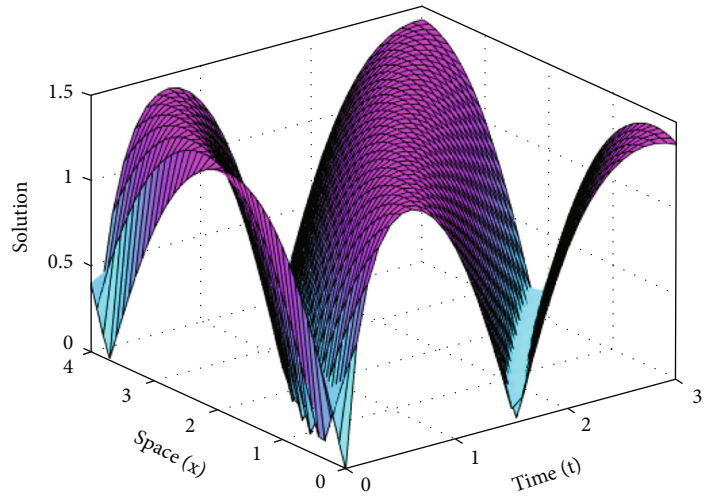

(b) $\alpha = 0.7, \sigma = 0.9$

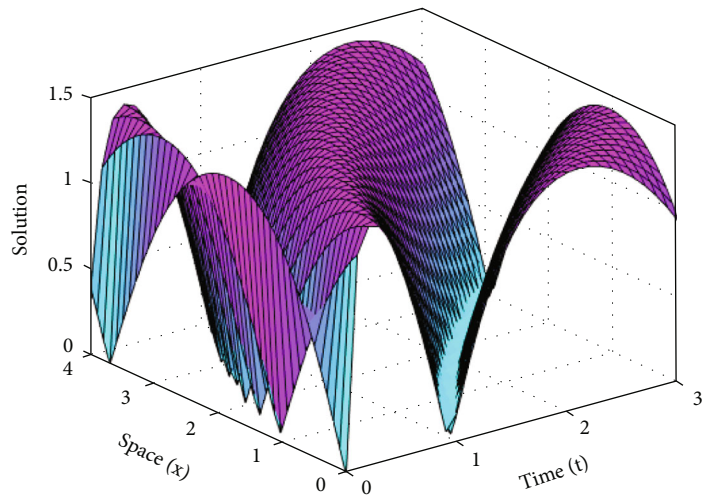

(c) $\alpha = 0.5, \sigma = 0.9$

Figure 4: Continued.

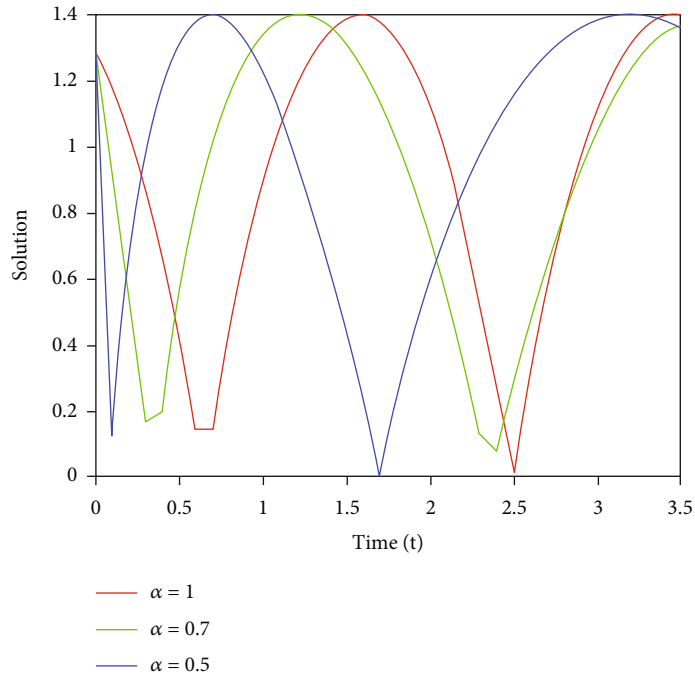

(d) $\alpha = 0.5$, 0.7, and 1

FIGURE 4: (a–c) 3D shape of Eq. (29) with $\alpha = 0.5$, 0.7, and 1. (d) 2D shape of Eq. (29) with vary values of α.

$$\Phi(x,t) = \pm\sqrt{\frac{-2}{B}}\left[\frac{(1-\kappa^2)}{\kappa cn(\eta_\alpha) + dn(\eta_\alpha)}\right]e^{i\mu_\alpha}, \text{ for } B < 0. \tag{59}$$

Hyperbolic solutions (if $\kappa \longrightarrow 1$ in (50)-(59) for $B > 0$)

$$\Phi(x,t) = \pm\sqrt{\frac{2}{B}}\coth(\eta_\alpha)e^{i\mu_\alpha}, \tag{60}$$

$$\Phi(x,t) = \pm\sqrt{\frac{1}{2B}}[\coth(\eta_\alpha) + \operatorname{csch}(\eta_\alpha)]e^{i\mu_\alpha}, \tag{61}$$

$$\Phi(x,t) = \pm\sqrt{\frac{2}{B}}\operatorname{csch}(\eta_\alpha)e^{i\mu_\alpha}. \tag{62}$$

Trigonometric solutions (if $\kappa \longrightarrow 0$ in (50)-(59) for $B > 0$)

$$\begin{aligned}
\Phi(x,t) &= \pm\sqrt{\frac{2}{B}}\tan(\eta_\alpha)e^{i\mu_\alpha},\\
\Phi(x,t) &= \pm\sqrt{\frac{2}{B}}\sec(\eta_\alpha)e^{i\mu_\alpha},\\
\Phi(x,t) &= \pm\sqrt{\frac{2}{B}}[\sec(\eta_\alpha) \pm \tan cn(\eta_\alpha)]e^{i\mu_\alpha},\\
\Phi(x,t) &= \pm\sqrt{\frac{1}{2B}}[\csc(\eta_\alpha) + \cot(\eta_\alpha)]e^{i\mu_\alpha},
\end{aligned} \tag{63}$$

where μ_α and η_α are defined in (14) or (15) in the sense of BD or MTD, respectively

Set 3. The solution of Eq. (19), utilizing Eqs. (22) and (27), is

$$\Psi(\eta_\alpha) = \left[\pm\sqrt{\frac{2p}{B}}\varphi(\eta_\alpha) \pm \sqrt{\frac{2r}{B}}\frac{1}{\varphi(\eta_\alpha)}\right], \text{for}\frac{p}{B}, \frac{r}{B} > 0. \tag{64}$$

Therefore, the solutions of FLE (2)/(3), by using Table 1, are as follows:

Elliptic solutions

$$\Phi(x,t) = \pm\sqrt{\frac{2}{B}}\left[\kappa sn(\eta_\alpha) + \frac{1}{sn(\eta_\alpha)}\right]e^{i\mu_\alpha}, \text{ for } B > 0, \tag{65}$$

$$\Phi(x,t) = \pm\sqrt{\frac{2}{B}}cs(\eta_\alpha) + \sqrt{\frac{2(1-\kappa^2)}{B}}\frac{1}{cs(\eta_\alpha)}\Bigg]e^{i\mu_\alpha}, \text{ for } B > 0, \tag{66}$$

$$\Phi(x,t) = \pm\sqrt{\frac{1}{2B}}\left[\frac{\kappa sn(\eta_\alpha}{dn(\eta_\alpha)+1} + \frac{dn(\eta_\alpha)+1}{sn(\eta_\alpha)}\right]e^{i\mu_\alpha}, \text{ for } B > 0, \tag{67}$$

$$\Phi(x,t) = \pm\sqrt{\frac{1-\kappa^2}{2B}}\left[\frac{cn(\eta_\alpha)}{sn(\eta_\alpha)+1} + \frac{sn(\eta_\alpha)+1}{cn(\eta_\alpha)}\right]e^{i\mu_\alpha}, \text{ for } B > 0, \tag{68}$$

$$\Phi(x,t) = \pm\sqrt{\frac{1}{2B}}\left[\frac{(1-\kappa^2)sn(\eta_\alpha)}{cn(\eta_\alpha)+dn(\eta_\alpha)} + \frac{cn(\eta_\alpha)+dn(\eta_\alpha)}{sn(\eta_\alpha)}\right]e^{i\mu_\alpha}, \text{ for } B > 0. \tag{69}$$

Hyperbolic solutions (if $\kappa \longrightarrow 1$ in (65)-(69))

$$\Phi(x,t) = \pm\sqrt{\frac{2}{B}}\tanh(\eta_\alpha) + \sqrt{\frac{2}{B}}\coth(\eta_\alpha)\Bigg]e^{i\mu_\alpha}, \text{ for } B > 0, \tag{70}$$

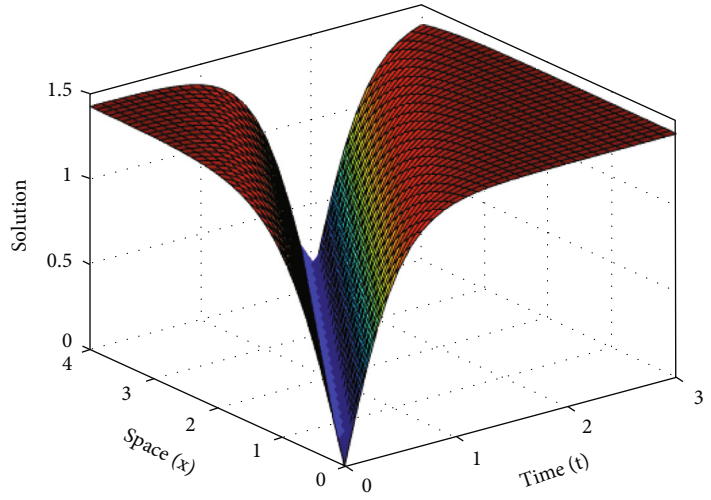

(a) $\alpha = 1, \sigma = 0$

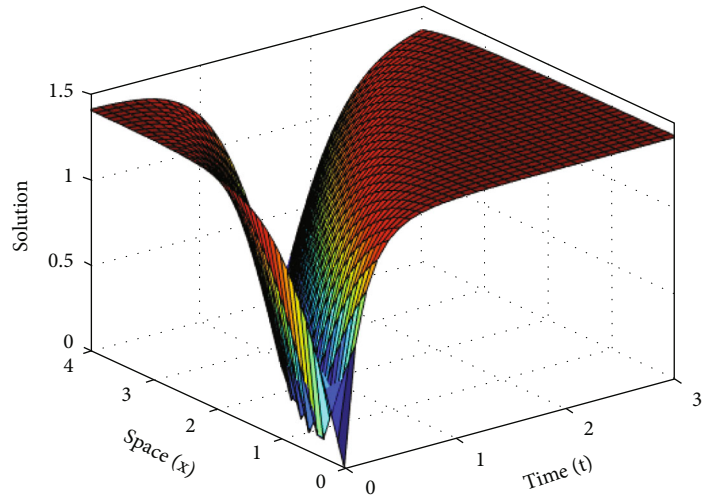

(b) $\alpha = 0.7, \sigma = 0.9$

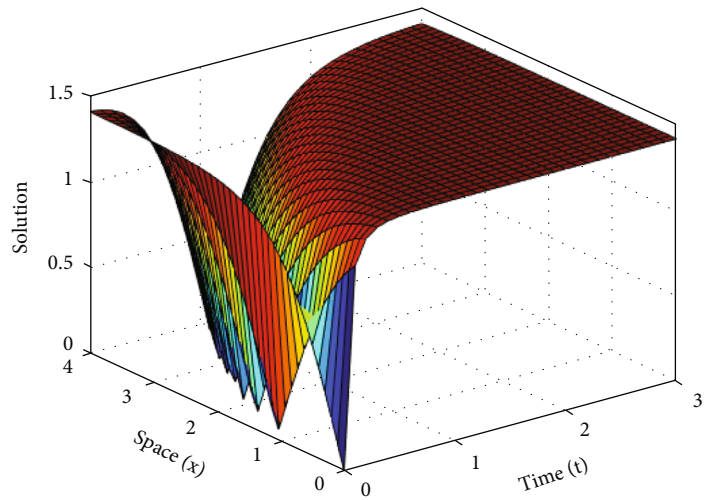

(c) $\alpha = 0.5, \sigma = 0.9$

Figure 5: Continued.

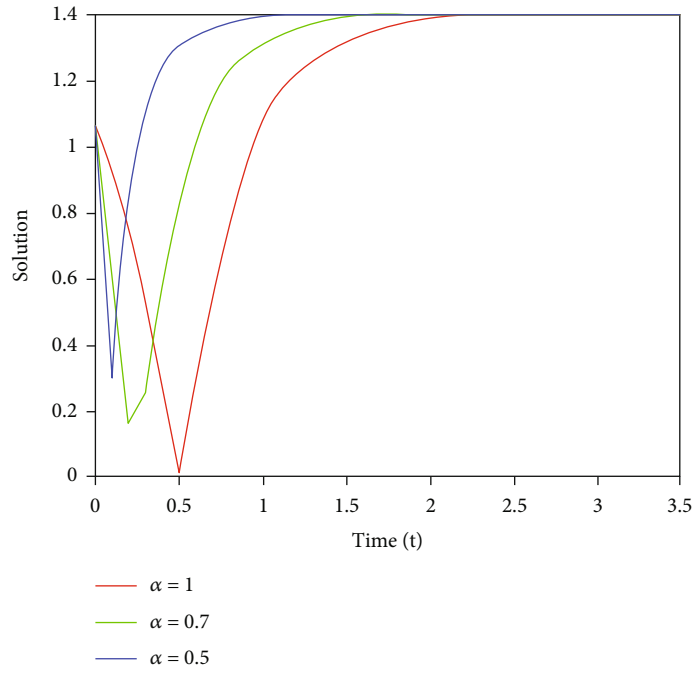

(d) $\alpha = 0.5$, 0.7, and 1

FIGURE 5: (a–c) 3D shape of Eq. (40) with $\alpha = 0.5$, 0.7, and 1. (d) 2D shape of Eq. (40) for distinct values of α.

$$\Phi(x,t) = \pm\sqrt{\frac{2}{B}}\coth(\eta_\alpha)e^{i\mu_\alpha}, \text{for } B > 0. \tag{71}$$

Trigonometric solutions (if $\kappa \longrightarrow 0$ in (65)-(69) for $B > 0$)

$$\begin{aligned}\Phi(x,t) &= \pm\sqrt{\frac{2}{B}}[\cot(\eta_\alpha) + \tan(\eta_\alpha)]e^{i\mu_\alpha},\\ \Phi(x,t) &= \pm\sqrt{\frac{2}{B}}\sec(\eta_\alpha)e^{i\mu_\alpha},\\ \Phi(x,t) &= \pm\sqrt{\frac{2}{B}}\csc(\eta_\alpha)e^{i\mu_\alpha},\end{aligned} \tag{72}$$

where μ_α and η_α are defined in (14) or (15) in the sense of BD or MTD, respectively

Remark 1. If we put $\alpha = 1$ (or $\alpha = 1$ and $\sigma = 0$) in Eq. (40), then we obtain the same results (71), respectively, reported in [24].

Remark 2. If we put $\alpha = 1$ (or $\alpha = 1$ and $\sigma = 0$) in Eqs. (60), (70), (44), and (41), then we get the same results (34), (35), (36), and (37), respectively, reported in [27].

6. Effects of the Beta and M-Truncated Derivatives

Now, we examine the effect of the BD and MTD on the obtained solutions of the FLE (2)/(3). A number of diagrams are presented to illustrate how these solutions behave. For specific achieved solutions including (29), (40), and (43), let us fix the parameters $\rho = \gamma_1 = \mu_1 = \eta_1 = 1$, $\eta_2 = 2$, $\mu_2 = -2$, $t \in [0, 2]$, and $x \in [0, 4]$ to plot these graphs.

6.1. The Effect of Beta Derivative. From Figures 1–3, we infer that all solution curves differ from one another. Furthermore, the surface shifts to the right as the order of the derivative decreases.

6.2. The Effect of M-Truncated Derivative. Finally, from Figures 4–6, we deduce that all solution curves are distinct from one another. Furthermore, the surface shifts to the left when the derivative's order decreases.

7. Results and Discussion

The Fokas-Lenells equation (FLE) is a nonlinear partial differential equation that arises in various fields of mathematical physics. It has several applications in fluid dynamics, quantum mechanics, and nonlinear optics, among others. Obtaining exact solutions for the FLE is of utmost importance. These solutions deepen our understanding of the physical phenomena, validate approximations and numerical methods, foster the development of new mathematical techniques, and facilitate education and training. The pursuit of exact solutions drives progress in mathematical physics and contributes to a broader scientific and technological advancement.

As a result, we obtained the exact solution for FLE including the M-truncated derivative or beta derivative. Utilizing the modified mapping method, new elliptic, hyperbolic, rational, and trigonometric solutions are acquired. For some fixed parameters and for various order of fractional

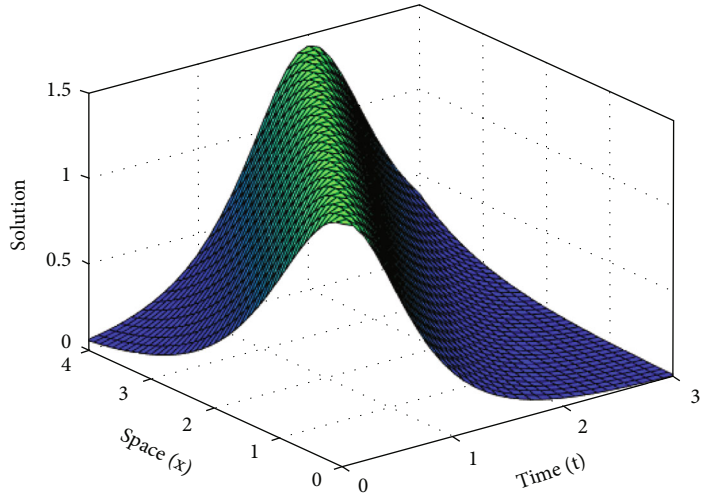

(a) $\alpha = 1, \sigma = 0$

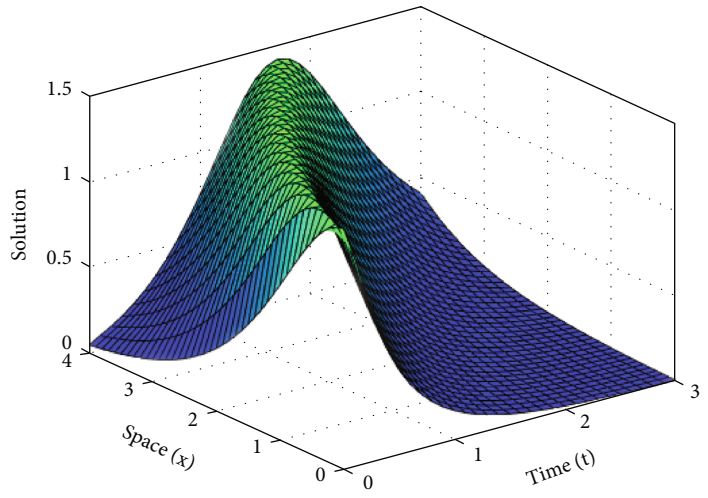

(b) $\alpha = 0.7, \sigma = 0.9$

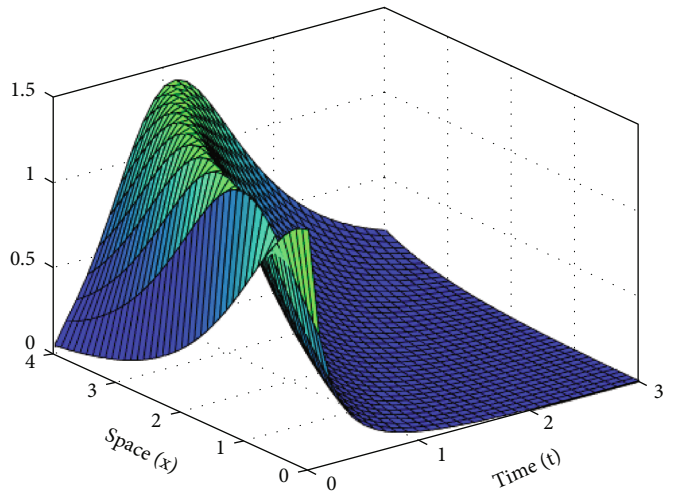

(c) $\alpha = 0.5, \sigma = 0.9$

Figure 6: Continued.

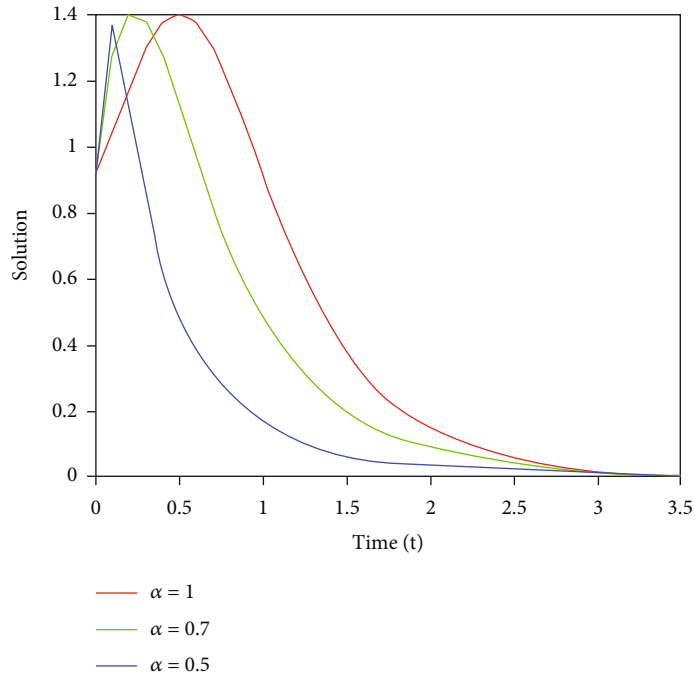

(d) $\alpha = 0.5$, 0.7, and 1

FIGURE 6: (a–c) 3D shape of Eq. (43) with $\alpha = 0.5$, 0.7, and 1. (d) 2D shape of Eq. (43) for various values of α.

derivatives, we plotted many graphs to display the impacts of fractional derivatives on the solutions. We deduced that when the derivative order decreases, the beta derivative pushes the surface to the left as shown in Figures 1–3, whereas the M-truncated derivative pushes the surface to the right as shown in Figures 4–6.

8. Conclusions

We looked at the Fokas-Lenells equation (FLE) with the beta and M-truncated derivatives. The exact solutions of FLE were acquired through the implementation of a modified mapping method. These results are vital in clarifying a broad variety of interesting and difficult physical processes. Furthermore, we extended some previous results such as the results stated in [24, 27]. In addition, the beta and M-truncated derivative impacts on the exact solution of FLE (2)/(3) were addressed by using the MATLAB program. Finally, we deduced that when the derivative order decreases, the beta derivative pushes the surface to the left, whereas the M-truncated derivative pushes the surface to the right. In future work, we look at Eq. (1) with additive noise.

Data Availability

All data are available in this paper.

Conflicts of Interest

The author declares that they have no competing interests.

Acknowledgments

This work is supported by the Princess Nourah bint Abdulrahman University Researcher Supporting Project (number PNURSP2023R 273), Princess Nourah bint Abdulrahman University, Riyadh, Saudi Arabia.

References

[1] M. Alshammari, A. E. Hamza, C. Cesarano, E. S. Aly, and W. W. Mohammed, "The analytical solutions to the fractional Kraenkel–Manna–Merle system in ferromagnetic materials," *Fractal and Fractional*, vol. 7, no. 7, p. 523, 2023.

[2] K. A. Gepreel and M. S. Mohamed, "An optimal homotopy analysis method nonlinear fractional differential equation," *Journal of Advanced Research in Dynamical and Control Sys tems*, vol. 6, pp. 1–10, 2014.

[3] K. Khan and M. A. Akbar, "The exp $(-\Phi(\varsigma))$-expansion method for finding travelling wave solutions of Vakhnenko-Parkes equation," *International Journal of Dynamical Systems and Differential Equations*, vol. 5, no. 1, pp. 72–83, 2014.

[4] A. M. Wazwaz, "The tanh method: exact solutions of the sine-Gordon and the sinh-Gordon equations," *Applied Mathematics and Computation*, vol. 167, no. 2, pp. 1196–1210, 2005.

[5] R. Hirota, "Exact solution of the Korteweg-de Vries equation for multiple collisions of solitons," *Physical Review Letters*, vol. 27, no. 18, pp. 1192–1194, 1971.

[6] Y. Pandir, Y. Gurefe, and E. Misirli, "A multiple extended trial equation method for the fractional Sharma-Tasso-Olver equation," *AIP Conference Proceedings*, vol. 1558, pp. 1927–1930, 2013.

[7] W. W. Mohammed, F. M. Al-Askar, and C. Cesarano, "Solutions to the (4+1)-dimensional time-fractional Fokas equation

with M-truncated derivative," *Mathematics*, vol. 11, no. 1, p. 194, 2023.

[8] F. M. Al-Askar, C. Cesarano, and W. W. Mohammed, "Abundant solitary wave solutions for the Boiti–Leon–Manna–Pempinelli equation with M-truncated derivative," *Axioms*, vol. 12, no. 5, p. 466, 2023.

[9] S. Kumar, D. Kumar, and H. Kharbanda, "Lie symmetry analysis, abundant exact solutions and dynamics of multisolitons to the (2+1)-dimensional KP-BBM equation," *Pramana*, vol. 95, no. 1, p. 33, 2021.

[10] S. Kumar and D. Kumar, "Lie symmetry analysis and dynamical structures of soliton solutions for the (2+1)-dimensional modified CBS equation," *International Journal of Modern Physics B*, vol. 34, no. 25, article 2050221, 2020.

[11] S. Kumar and S. Rani, "Lie symmetry reductions and dynamics of soliton solutions of (2 +1)-dimensional Pavlov equation," *Pramana*, vol. 94, no. 1, p. 116, 2020.

[12] W. W. Mohammed, C. Cesarano, and E. S. Aly, "The soliton solutions of the stochastic shallow water wave equations in the sense of beta-derivative," *Mathematics*, vol. 11, no. 6, p. 1338, 2023.

[13] S. Kumar, N. Mann, H. Kharbanda, and M. Inc, "Dynamical behavior of analytical soliton solutions, bifurcation analysis, and quasi-periodic solution to the (2+1)-dimensional Konopelchenko–Dubrovsky (KD) system," *Analysis and Mathematical Physics*, vol. 13, no. 3, p. 40, 2023.

[14] E. Az-Zo'bi, A. F. Al-Maaitah, M. A. Tashtoush, and M. S. Osman, "New generalised cubic–quintic–septic NLSE and its optical solitons," *Pramana*, vol. 96, no. 4, p. 184, 2022.

[15] E. Az-Zo'bi, L. Akinyemi, and A. O. Alleddawi, "Construction of optical solitons for conformable generalized model in nonlinear media," *Modern Physics Letters B*, vol. 35, no. 24, article 2150409, 2021.

[16] R. U. Rahman, W. A. Faridi, M. A. El-Rahman, A. Taishiyeva, R. Myrzakulov, and E. A. Az-Zo'bi, "The sensitive visualization and generalized fractional solitons' construction for regularized long-wave governing model," *Fractal and Fractional*, vol. 7, no. 2, p. 136, 2023.

[17] W. W. Mohammed and D. Blömker, "Fast-diffusion limit for reaction-diffusion equations with multiplicative noise," *Journal of Mathematical Analysis and Applications*, vol. 496, no. 2, article 124808, 2021.

[18] M. L. Wang, X. Z. Li, and J. L. Zhang, "The (G'G)-expansion method and travelling wave solutions of nonlinear evolution equations in mathematical physics," *Physics Letters A*, vol. 372, no. 4, pp. 417–423, 2008.

[19] F. M. Al-Askar, C. Cesarano, and W. W. Mohammed, "The analytical solutions of stochastic-fractional Drinfel'd-Sokolov-Wilson equations via (G'/G)-Expansion method," *Symmetry*, vol. 14, no. 10, p. 2105, 2022.

[20] G. Tao, J. Sabi'u, S. Nestor et al., "Dynamics of a new class of solitary wave structures in telecommunications systems via a (2+1)-dimensional nonlinear transmission line," *Modern Physics Letters B*, vol. 36, no. 19, article 2150596, 2022.

[21] W. W. Mohammed, F. M. Al-Askar, and M. El-Morshedy, "Impact of multiplicative noise on the exact solutions of the fractional-stochastic Boussinesq-Burger system," *Journal of Mathematics*, vol. 2022, Article ID 9288157, 2022.

[22] S. Alshammari, W. W. Mohammed, S. K. Samura, and S. Faleh, "The analytical solutions for the stochastic-fractional Broer–Kaup equations," *Mathematical Problems in Engineering*, vol. 2022, Article ID 6895875, 9 pages, 2022.

[23] M. Inc, E. A. Az-Zo'bi, A. Jhangeer, H. Rezazadeh, M. N. Ali, and M. K. A. Kaabar, "New soliton solutions for the higher-dimensional non-local Ito equation," *Nonlinear Engineering*, vol. 10, no. 1, pp. 374–384, 2021.

[24] S. T. Demiray and H. Bulut, "New exact solutions of the new Hamiltonian amplitude-equation and Fokas Lenells equation," *Entropy*, vol. 17, no. 12, pp. 6025–6043, 2015.

[25] J. Xu and E. Fan, "Leading-order temporal asymptotics of the Fokas-Lenells equation without solitons," 2013, https://arxiv.org/abs/1308.0755.

[26] P. Zhao, E. Fan, and Y. Hou, "Algebro-geometric solutions and their reductions for the Fokas-Lenells hierarchy," *Journal of Nonlinear Mathematical Physics*, vol. 20, no. 3, pp. 355–393, 2013.

[27] A. F. Aljohani, E. R. El-Zahar, A. Ebaid, M. Ekici, and A. Biswas, "Optical soliton perturbation with Fokas-Lenells model by Riccati equation approach," *Optik-International Journal for Light and Electron Optics*, vol. 172, pp. 741–745, 2018.

[28] H. Bulut and B. J. Khalid, "Optical soliton solutions of Fokas-Lenells equation via (m +1/G')- expansion method," *Journal of Advances in Applied & Computational Mathematics*, vol. 7, pp. 20–24, 2020.

[29] H. Triki and A. Wazwaz, "Combined optical solitary waves of the Fokas—Lenells equation," *Waves in Random and Complex Media*, vol. 27, no. 4, pp. 587–593, 2017.

[30] E. V. Krishnan, A. Biswas, Q. Zhou, and M. Alfiras, "Optical soliton perturbation with Fokas–Lenells equation by mapping methods," *Optik*, vol. 178, pp. 104–110, 2019.

[31] U. N. Katugampola, "New approach to a generalized fractional integral," *Applied Mathematics and Computation*, vol. 218, no. 3, pp. 860–865, 2011.

[32] U. N. Katugampola, "New approach to generalized fractional derivatives," *Bulletin of Mathematical Analysis and Applications*, vol. 6, no. 4, pp. 1–15, 2014.

[33] A. A. Kilbas, H. M. Srivastava, and J. J. Trujillo, *Theory and Applications of Fractional Differential Equations*, Elsevier, Amsterdam, Netherlands, 2016.

[34] S. G. Samko, A. A. Kilbas, and O. I. Marichev, *Fractional Integrals and Derivatives, Theory and Applications*, Gordon and Breach, Yverdon, Switzerland, 1993.

[35] A. Atangana, D. Baleanu, and A. Alsaedi, "Analysis of time-fractional Hunter-Saxton equation: a model of neumatic liquid crystal," *Open Physics*, vol. 14, no. 1, pp. 145–149, 2016.

[36] J. V. Sousa and E. C. de Oliveira, "A new truncated Mfractional derivative type unifying some fractional derivative types with classical properties," *International Journal of Analysis and Applications*, vol. 16, pp. 83–96, 2018.

[37] A. H. Bhrawy, M. A. Abdelkawy, S. Kumar, S. Johnson, and A. Biswas, "Solitons and other solutions to quantum Zakharov–Kuznetsov equation in quantum magneto-plasmas," *Indian Journal of Physics*, vol. 87, no. 5, pp. 455–463, 2013.